# Enzyme-based Electrochemical Biosensor for Therapeutic Drug Monitoring of Anticancer Drug Irinotecan

Maria Domenica Alvau, Stefano Tartaggia, Anna Meneghello, Bruno Casetta, Giammario Calia, Pier Andrea Serra, Federico Polo, and Giuseppe Toffoli

*Anal. Chem.*, **Just Accepted Manuscript** • DOI: 10.1021/acs.analchem.7b04357 • Publication Date (Web): 16 Apr 2018

# Enzyme-based Electrochemical Biosensor for Therapeutic Drug Monitoring of Anticancer Drug Irinotecan

Maria Domenica Alvau,[a,‡] Stefano Tartaggia,[a,‡] Anna Meneghello,[a] Bruno Casetta,[a] Giammario Calia,[b] Pier Andrea Serra,[b] Federico Polo,[a,*] Giuseppe Toffoli[a]

[a]Experimental and Clinical Pharmacology Division, CRO Aviano - National Cancer Institute, Italy

[b]Department of Clinical and Experimental Medicine section of Pharmacology, University of Sassari, Viale San Pietro 43/b, Sassari, Italy

*Corresponding author

E-mail: federico.polo@cro.it

Phone: +39 0434 659816

**ABSTRACT:** Therapeutic drug monitoring (TDM) is the clinical practice of measuring pharmaceutical drug concentrations in patients' biofluids at designated intervals, thus allowing a close and timely control of their dosage. To date, TDM in oncology can only be performed by trained personnel in centralized laboratories and core facilities employing conventional analytical techniques (e.g. MS). CPT-11 is an antineoplastic drug that inhibits topoisomerase type I, causing cell death, and is widely used in the treatment of colorectal cancer. CPT-11 was also found to directly inhibit acetylcholine esterase (AChE), an enzyme involved in neuromuscular junction. In this work, we describe an enzymatic biosensor, based on AChE and Choline oxidase (ChOx), which can quantify CPT-11. ACh (acetylcholine) substrate is converted to choline, which is subsequently metabolized by ChOx to give betaine aldehyde and hydrogen peroxide. The latter one is then oxidized at a suitably polarized platinum electrode, providing a current transient proportional to the amount of ACh. Such enzymatic process is hampered by CPT-11. The biosensor showed a ~60% maximal inhibition towards AChE activity in the clinically relevant concentration range 10-10,000 ng/mL of CPT-11 in both simple (phosphate buffer) and complex (fetal bovine serum) matrices, while its metabolites showed negligible effects. These findings could open new routes towards a real-time TDM in oncology, thus improving the therapeutic treatments, and lowering the related costs.

*Biosensor, Therapeutic Drug Monitoring, Chemotherapeutic Drug, Irinotecan, Acetylcholine Esterase.*

Therapeutic drug monitoring (TDM) is the clinical practice of measuring pharmaceutical drug concentrations in patients' biofluids at designated intervals allowing a close and timely control of their dosage. The main advantage of TDM is the rapid medical intervention in case of toxicity-related issues and/or adjustment of dosage to better fit the therapeutic demand.[1]

It becomes particularly important in the treatment of cancer diseases, since antineoplastic drugs often show a narrow therapeutic range (the concentration range in between non-efficacy and toxicity), which might cause under dosage and subsequent therapeutic failure, or over dosage and therefore severe adverse effects.

Once the clinical conditions of the patients are assessed, along with individual characteristics, such as weight, age, and other concomitant drug therapy, an initial dosage regimen is determined and TDM begins. In fact, each patient might respond differently to the same therapy, given that the pharmacokinetics of any drug depends on the metabolic processes of each individual.

Currently, TDM in oncology is performed in centralized laboratories and core facilities within specific clinical research programs, still far from the routine practice. Conventional instruments, such as mass spectrometer (MS), are employed, which can be run only by qualified and trained personnel. Moreover, the time required to collect, process and analyze the samples, and to process the results, together with the related financial cost, severely limits the application of TDM in medical practices. Therefore, a new generation of analytical tools is necessary to respond to the timely need of drug administration or reduction aiming at effectively treating cancer patients.[2,3]

Colorectal cancer is the third most common form of cancer worldwide, it also represents the second major cause

of death in both male and female patients, accounting for 9.4% of all incident cancer in men and 10.1% in women. It was estimated that about 850,000 new cases and 500,000 deaths occur yearly worldwide.[4,5]

Irinotecan (7-ethyl-10-[4-(1-piperidino)-1-piperidino]-carbonyloxycamptothecine), namely CPT-11, is derived from the natural alkaloid camptothecine, and is widely used in the treatment of colorectal cancer. [6–9]

CPT-11 is in fact a pro-drug, which is metabolized in the liver and converted in its active form, 7-ethyl-10-hydroxycamptothecin (SN-38), by the liver carboxylase (CE),[6,10–13] as summarized in Scheme1. Following the metabolic pathway, SN-38 is then converted into 7-Ethyl-10-hydroxy-camptothecin-10-O-β-D-glucuronide(SN38-G), by hepatic UDP-glucuronyltransferase (UGT1A1/7), and finally excreted through urine.[14,15] Several metabolites of CPT-11 were also identified, which include 7-ethyl-10-[4-N-(5-aminopentanoic acid)-1-piperidino]carbonyloxycamptothecin (APC) and 7-ethyl-10-(4-amino-1-piperidino)carbonyloxycamptothecin (NPC), which are generated by cytochrome P-450 3A4 (CYP3A4).[12,13,16,17] Other minor metabolites, whose metabolic pathways and biologic activities have not been identified yet, also exist.[16]

**Scheme1. Metabolic pathway of CPT-11 and its main metabolites.**

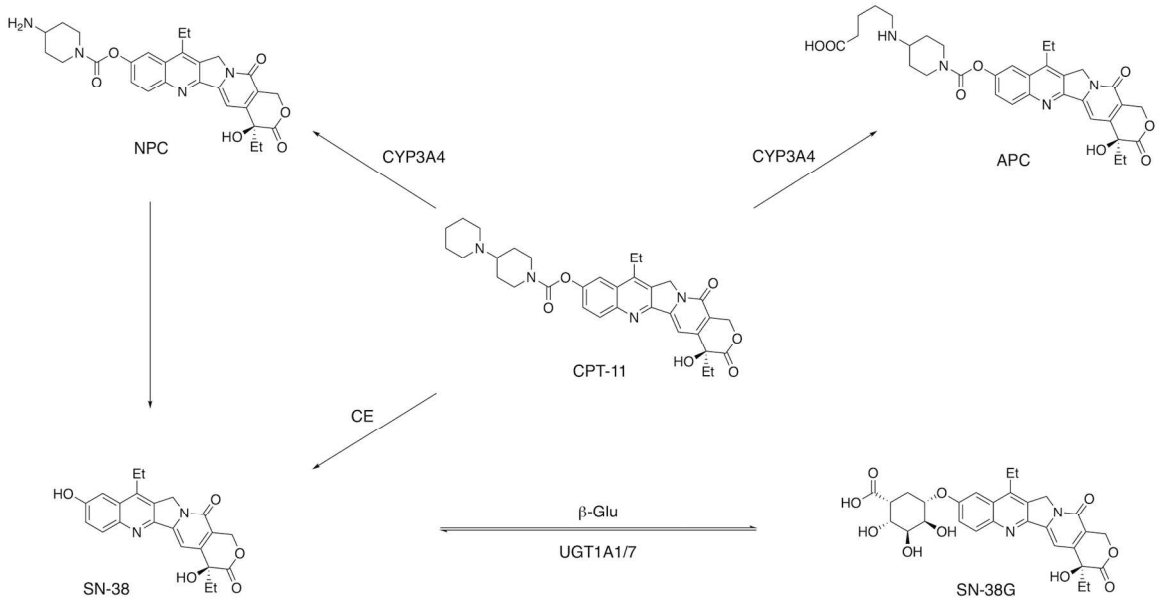


SN-38 irreversibly inhibits the nuclear enzyme topoisomerase type I (Topo-I), which is involved in the relaxation of supercoiled DNA,[18] and plays a key role during replication, recombination, transcription, and reparation of DNA. Its inhibition by SN-38 triggers the tumor cell death through apoptosis.[10]

Typically, the levels of SN-38 in patients treated with irinotecan are about 100-fold lower than irinotecan. However, such concentrations are relevant, as SN-38 is up to 1000-fold more cytotoxic than the parent compound.[13]

To date, there is no clinical instrumentation devised to detect and monitor the levels of CPT-11 in biofluids during therapeutic treatment. This would be extremely useful to help a prompt medical intervention, thus avoiding severe adverse effects while administering the therapy, therefore effectively ameliorating the quality of life of oncological patients and reducing the costs for the Healthcare System.[19]

So far, few examples of biosensors were reported to detect CPT-11 through optical and/or electrochemical methodologies. Among them it is worth to mention an enzymatic biosensor that exploits the interaction of CPT-11 with Topo-I, immobilized on a gold chip, to determine the anticancer drug *via* surface plasmon resonance (SPR).[20] Another type of biosensor, which was based on the interaction between the drug and DNA-modified electrodes, allowed quantification of CPT-11 through cyclic and differential pulse voltammetry.[21] Both examples, performed in buffer, were not aimed at TDM or clinical application, but at the analysis of specific molecular interaction mechanisms.

Other devices were developed, which employed the thin layer chromatography coupled with gold and silver nanoparticles for Raman-SERS detection.[22,23]

In addition to the Topo-I inhibition activity, CPT-11 directly inhibits acetyl cholinesterase (AChE), which occasionally produces acute cholinergic side effects.[24,25,17] *In vitro* experiments showed the inhibition effect of CPT-11 toward the active site of different AChE isoforms.[26]

AChE, which metabolizes the neurotransmitter acetylcholine, is found in the neuronal muscular junction and in the central nervous system. Biosensors employing the enzyme AChE were first developed as colorimetric assay to detect organophosphoric poison or pesticide in food and environmental samples, since this kind of molecules are known to have an inhibitory effect on AChE.[27] Biosensors, relying on the same enzymatic mechanism, were also successfully employed to detect therapeutics used in the

treatment of Alzheimer's disease.[28] Other electrochemical biosensors were developed, where AChE was directly immobilized on electrodes, suitably modified with gold nanoparticles-polypyrrole nanowires,[29] platinum nanoparticles-graphene-nafion.[30] However, to the best of our knowledge, to date no clinical applications in oncology and chemotherapeutics of the above-mentioned biosensors have been reported.

Herein we describe the development of an enzyme-based electrochemical biosensor aimed at detecting and quantifying the antineoplastic pro-drug CPT-11 in the concentration range 10-10,000 ng/ml, which is typically found in plasma sample of patients under chemotherapeutic treatment.[31] Taking advantage of the inhibition capability of irinotecan towards AChE, the biosensor was devised by employing the enzyme couple AChE/ChOx.

Few examples of biosensors employing this enzymatic couple were developed to determine the inhibition effect of some chemicals towards AChE.[28,32–36] Upon addition of a suitable amount of ACh, the following enzymatic reactions take place at the sensor surface (Scheme 2):

**Scheme 2. Enzymatic reactions involving AChE and ChOx**

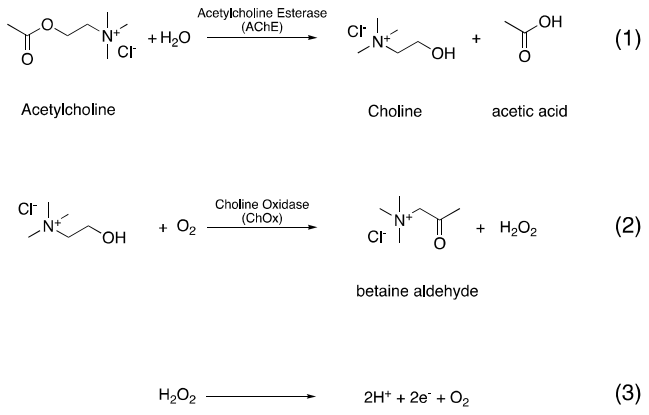


Acetylcholine is converted to choline and acetic acid by AChE (1). Choline becomes the substrate for ChOx, which oxidizes it to betaine aldehyde and hydrogen peroxide (2). The latter one can be amperometrically detected at the surface of a suitably polarized electrode (3). In fact, hydrogen peroxide is electrooxidized, thus providing a current transient, whose intensity is related to the original concentration of ACh.

The inhibition mechanism involving CPT-11 is hampering the first enzymatic reaction (1), thus reducing the amount (or even avoiding its formation) of available choline (2), and therefore $H_2O_2$ (3). The outcome is a decrease of the current intensity. Such inhibition allows for an indirect quantification of CPT-11 present in the sample.

## EXPERIMENTAL SECTION

The chemicals used in this work, mass spectrometry work station and other experimental details, metabolic pathway for CPT-11, and Michaelis-Menten kinetics for the electrochemical biosensors are provided in the Supporting Information.

**Biosensor Fabrication.** The Teflon insulation was removed from Teflon-coated platinum wires (Advent Research Materials), and bare platinum electrodes (1 mm length and 125 μm diameter) were then immersed into a freshly prepared *ortho*-phenyldiamine (oPD) solution (300 mM). A constant potential of +0.7 V versus Ag/AgCl was then applied for 30 min to form a polymeric film of polyphenyldiamine (PPD). The electrode wire was then washed with bidistilled water and dipped at room temperature (25 ºC) into a solution containing 20 U $ml^{-1}$ (0.52 mM) of AChE and 10 U $ml^{-1}$ (0.2 mM) of ChOx for 5 minutes, and then into a solution of polyethyleneimine (PEI) 1% (w/v). According to specific sensor design, the electrode wires were dip coated into the enzyme couple and then PEI solutions, followed by 5 minutes dip coating into BSA 2% solution and finally by 5 minutes into 1% glutaraldehyde (GA) solution, which was allowed to dry at 37 ºC for 15 minutes.[36–38] A schematic representation of the biosensor is shown in Scheme 3 and discussed in the following section.

Taking into account the procedure described above, the sensors were prepared according to the following design scheme: Pt/PPD/[AChE-ChOx + PEI(1%)]$_z$/BSA(2%)$_1$/GA(1%)$_1$, where $z$ is the number of dip coatings into the enzyme couple and PEI solutions. Ten types of sensors (**1**-**10**) were prepared (see Supporting Information).

**Electrochemistry.** A platinum wire served as counter electrode, and a Ag/AgCl chloride wire was used as reference electrode. The chronoamperometry experiments were carried out in PBS and FBS solutions, employing a three-electrode configuration electrochemical cell. A CHI 1040C electrochemical workstation (CH Instruments, Austin, TX, USA) was used. Each biosensor design **1**-**10** was tested and characterized with the substrate acetylcholine. The enzymatic reaction, which was found to follow the Michaelis-Menten kinetics (see Supporting Information for further details), was evaluated by adding increasing concentrations of acetylcholine to PBS or FBS solutions. A non-linear regression of the data plot, according to the Michaelis-Menten, was performed to evaluate the kinetic parameters, $V_{Max}$ and $K_M$.

Concerning the detection of the analyte, once the biosensors were activated with ACh, increasing concentration of CPT-11 were injected in PBS or FBS solutions to determine the extent of inhibition of the antineoplastic drugs toward the AChE, and a calibration plot was then obtained. The same procedure was also performed for CPT-11 metabolites.

**Statistical Analysis.** The response of biosensors toward ACh and CPT-11 was evaluated at day 1, right after fabrication. Each current step response was averaged over 100 data points, upon each addition of ACh or CPT-11. The concentration range for ACh was 5 μM-10 mM, while for CPT-11 was 16 nM-16 μM, obtained from stock solutions in PBS and FBS at room temperature (25 °C). Statistical analysis was performed with Graphpad Prism® (La Jolla, CA, USA), which allowed calculating Michaelis-Menten parameters ($V_{Max}$ and $K_M$.), $IC_{50}$ and the extent of enzyme inhibition. As described in Supporting Information (equation 2), $K_M$ and $V_{Max}$ were calculated by employing the Michaelis-Menten kinetics, expressed in terms of current response. To evaluate the inhibition effect of the anticancer drugs toward the

enzymatic activity, a 100% enzymatic activity was assumed before the addition of the drugs.

Limit of detection (LOD) and limit of quantification (LOQ) were evaluated by using the equations LOD = $3s_b/A$ and LOQ = $10s_b/A$, where $s_b$ is the standard deviation of the blank and A is the slope of the calibration curve.[39,40] $IC_{50}$ is the inhibitor concentration needed to reach 50% enzymatic activity inhibition.

## RESULTS AND DISCUSSION

**Biosensors Characterization.** The biosensors were prepared as described in the Experimental Section, according to the designs **1-10** and following the procedure previously described by us.[36–38] A schematic representation of the biosensor is shown in Scheme 3. The difference between the designs **1-10** (for details, see Supporting Information) is the amount of enzymes and PEI layers, due to the increased number of dip coatings in the corresponding solutions, whereas albumin and glutaraldehyde content remain constant.

**Scheme 3. Biosensor design and working principle.**

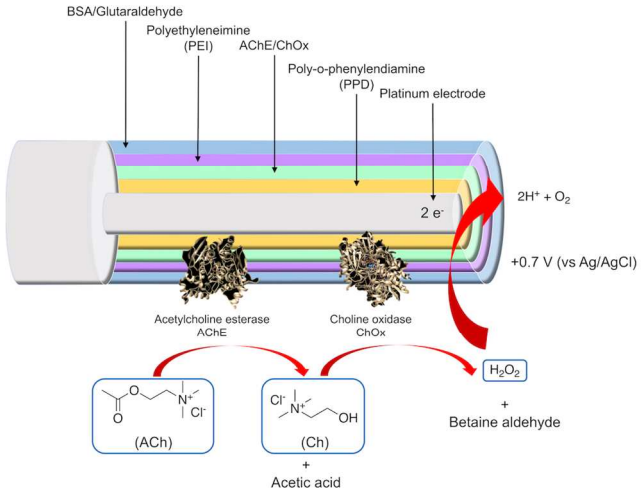


All biosensor designs were calibrated with the substrate ACh in the concentration range 5 µM-10 mM, both in simple (PBS) and complex (FBS) matrix solutions. As it will be described later in this section, design **5** proved to be the best-performing.

Figure 1 shows the response of the biosensor (red plot) and the negative control (blue plot), provided by a dummy biosensor, toward ACh addition in the concentration range 5 µM-10 mM. The latter one contains only ChOx enzyme and was prepared to assess (i) the specificity of the system toward ACh, and (ii) the role played by interferences, which might be present in the matrices (matrix effect).

The biosensor and the negative control were inserted in the electrochemical cell containing the electrolyte solution (PBS or FBS) and a constant potential of +0.7 V (vs Ag/AgCl reference electrode) was applied to record the chronoamperometric profile. Once the current transient was stable (typically 10-15 minutes), ACh was added in solution, and the cascade of enzymatic reactions, described by (1) and (2), immediately took place. Hydrogen peroxide was then immediately oxidized at the platinum electrode (3), thus making the current increase. Each addition of ACh in solution corresponded to an increase in the current response that reached the steady state when ACh concentration reached 10 mM, as shown in Figure 2.

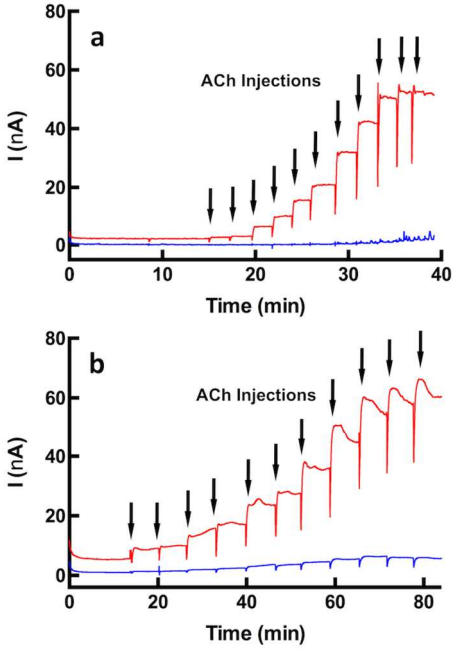


**Figure 1**. Chronamperometric profile for the calibration of the biosensor design 5 (red line) and dummy biosensor (blue line) with the substrate ACh in (a) PBS and (b) FBS. ACh was sequentially added in solution (black arrows) to reach the following concentrations: (from left to right) 0.005, 0.01, 0.05, 0.1, 0.2, 0.5, 1, 2, 3, 5, 10 mM.

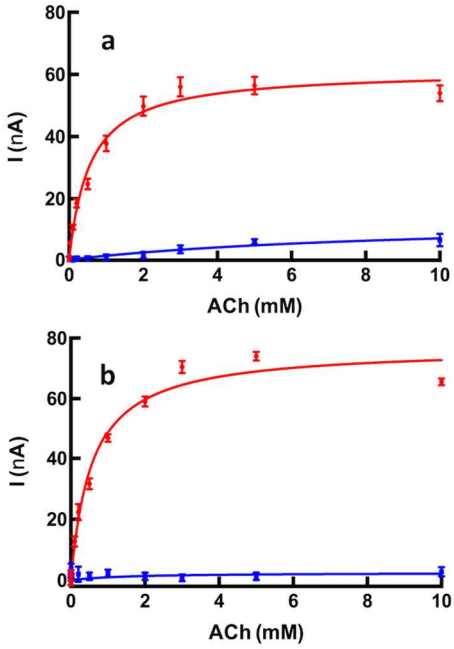


**Figure 2.** Michaelis–Menten kinetics plot for biosensor design 5 in (a) PBS and (b) FBS are also shown.

Upon evaluation of the Michaelis-Menten kinetics, the parameters $V_{Max}$ and $K_M$ were calculated, and their values are reported for PBS in Table 1.

**Table 1. $V_{Max}$ and $K_M$ values in PBS for biosensors 1-10.**

| Design | $V_{Max}$ (nA) | $K_M$ (μM) |
|---|---|---|
| 1 | 40.55±4.54 | 2.32±0.65 |
| 2 | 27.83±2.72 | 1.32±0.38 |
| 3 | 25.10±2.53 | 1.57±0.44 |
| 4 | 28.80±2.88 | 1.33±0.39 |
| 5 | 61.85±2.53 | 0.58±0.09 |
| 6 | 57.32±5.88 | 0.94±0.31 |
| 7 | 23.88±5.35 | 12.24±0.42 |
| 8 | 18.56±5.04 | 15.54±6.07 |
| 9 | 23.68±4.98 | 10.74±3.58 |
| 10 | 25.01±5.81 | 10.39±3.86 |

Furthermore, acetaminophen, which might be also administered during the chemotherapeutic regimen as pain and fever relief, was also tested, since it can be oxidized at a potential close to that of hydrogen peroxide. The results (see Supporting Information, Figure S1) showed a negligible effect due to acetaminophen, thus indicating that the poly-o-phenylendiamine layer shielded the platinum electrode, without preventing hydrogen peroxide to be oxidized, as previously described with respect to other interferences, such as ascorbic acid.[36,37]

PBS is commonly used as media for biosensing, whereas FBS offers an excellent surrogate of a biological environment to test and improve the biosensor performances, in view of its application to human samples and TDM implementation within clinical practice. Our findings indicate that, under optimized experimental conditions, the biosensors **5** show similar performances in both simple and complex matrices. In fact, $V_{Max}$ is 61.8±0.25 nA (PBS) and 76.9±0.34 nA (FBS), while $K_M$ is 0.58±0.09 μM (PBS) and 0.57±0.10 μM (FBS), thus indicating that the matrix effect on the biosensor performance is negligible. Similar results were obtained for the other biosensor designs.

The biosensors were tested to assess which design was the best performing in terms of sensitivity and dynamic range. The test was performed only in PBS. Two parameters were taken into account: (i) the amount of enzymes necessary to provide a measurable signal (hydrogen peroxide produced during the enzymatic reaction) and (ii) the amount of ACh required to activate and to calibrate the biosensor in the CPT-11 concentration range of interest for clinical application (10-10,000 ng/ml). These parameters mainly depend on the values of $V_{Max}$ and $K_M$. In particular, the latter one plays an important role since it determines both the amplitude of the linear region slope (LRS = $V_{Max}/K_M$), and the concentration range in the linear response (~$1/2K_M$).[41]

The higher the $K_M$ the lower the affinity of the enzyme for the substrate.[42] In this case, binding of CPT-11 may also occur to unsaturated AChE sites that would not result in any measurable inhibition, since the ACh hydrolysis would not be hampered. Instead, the lower the $K_M$, the higher the affinity of the enzyme for the substrate ACh and the wider the LRS, so that the biosensor reaches saturation very rapidly. Therefore, the optimal condition to assess AChE inhibition by CPT-11 is within the linear region of Michaelis-Menten plot (see Figure S2). On the other hand, a high value for $V_{Max}$ also helps increasing the LRS, and a lower concentration of ACh is required to reach saturation, thus enhancing the observable inhibition effect by CPT-11.

As reported in Table 1 and shown in Figure 3, **5** proved to be the best performing sensor design, since it showed the lower and the highest values for $K_M$ and $V_{Max}$, respectively. In fact, $K_M$ decreased from design 1 to reach a minimum value for design 5, and then increased again from design **6** to **10**. while $V_{Max}$ showed an opposite trend. We hypothesize that the amount of enzymes on the biosensor can be conveniently increased to optimize $K_M$ and $V_{Max}$ to the point where a higher concentration of enzymes in the biosensors hamper the normal enzymatic activity, which then decrease. Design **5** was therefore selected for all subsequent experiments.

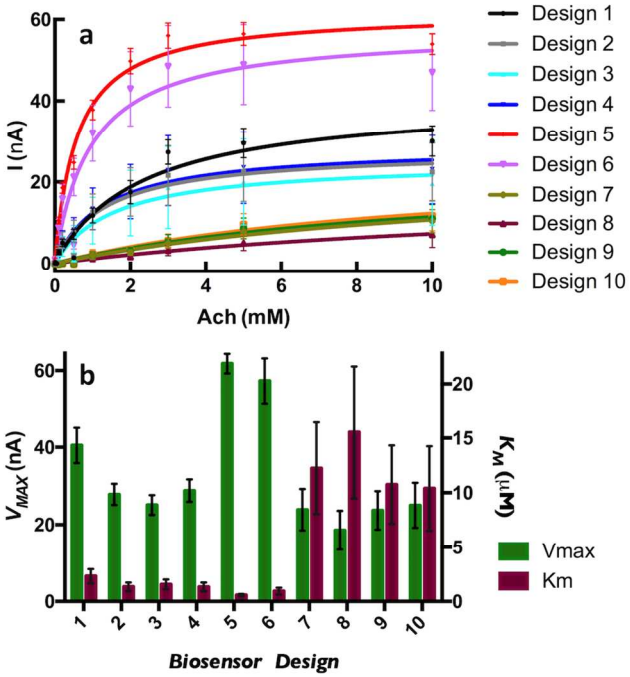


**Figure 3.** (a) Michaelis–Menten kinetics plot for biosensor designs **1-10**. (b) Histograms representing the $V_{Max}$ (green bars) and $K_M$ (dark red bars) for biosensor designs **1-10.**

**Biosensor specificity towards CPT-11 and its metabolites.** Upon activation of the biosensor with one single injection of ACh (30 μM), the current increased due to the oxidation of hydrogen peroxide. Once the current transient stabilized, CPT-11 was added in solution and inhibition of AChE occurred immediately, thus causing the decrease of hydrogen peroxide concentration, proportionally to the amount of antineoplastic drug (see Figure 4). As a consequence, the current also decreased stepwise upon each

consecutive addition of CPT-11. Figure 4b shows a zoom-in of the chronoamperometric profile upon sequential addition of CPT-11 to better appreciate the current decrease, whose order of magnitude is in the high pA range (0.14±0.04 nA) per each step. Multiple additions of CPT-11 in the solution then allowed for the calibration of the sensor. Characterization was performed in PBS and FBS solutions in the concentration range 10-10,000 ng/ml (16 nM-16 μM), which is usually found in the plasma of patients under therapeutic regimen.[31]

Concerning the amount of ACh, 30 μM was chosen within the LRS to activate and to calibrate the biosensor. However, it is worth noting that a higher concentration of ACh (e.g. 50 μM) would have caused the initial current change to be so intense that the subsequent current steps, related to the CTP-11 injections, would have been negligible compared to the baseline (data not shown).

Our results also showed (Figure 5a) that the residual activity of AChE was 40.6±4.5 % (PBS) and 39.9±3.5 % (FBS) when the concentration of CPT-11 reached its maximum value (10,000 ng/ml). Concerning $IC_{50}$, values of 0.47 μM (295 ng/ml) in PBS and 0.43 μM (268 ng/ml) in FBS were obtained.

A linear calibration curve was obtained (Figure 5b), by plotting the value for each current step, obtained from the average of 8 biosensors working in parallel, against the logarithm of CPT-11 concentration. The plot also showed a higher sensitivity for CPT-11 in FBS (-1.59±0.08) than PBS (-0.59±0.07), therefore evidencing a better response of the biosensor operating in a biological matrix rather than simple PBS buffer.

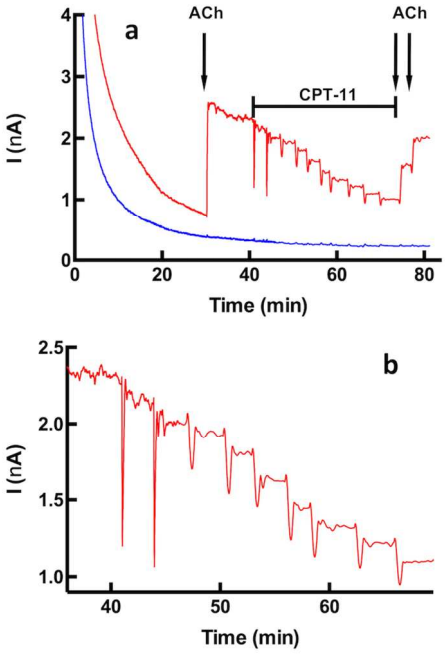


**Figure 4.** (a) Full chronoamperometric profile related to the biosensor calibration with CPT-11 (red plot) with respect to the dummy biosensor (blue plot). 30 μM ACh was used to activate the biosensor, subsequently CPT-11 was added in the concentration range 10-10,000 ng/ml. (b) Zoom-in of the chronoamperometric profile related to CPT-11 addition.

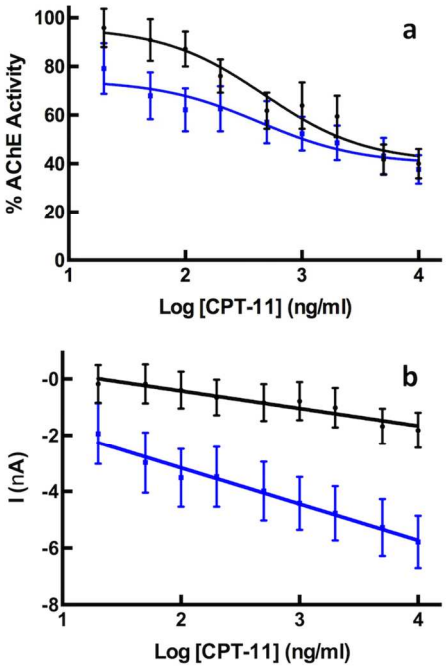


**Figure 5.** (a) Residual activity of AChE in PBS (black line) and FBS (blue line) after sequential addition of CPT-11. (b) Calibration plot for CPT-11 in PBS (black line) and FBS (blue line).

Moreover, we found LODs of 1.6 ng/ml and 1.5 ng/ml, and LOQs of 4.7 ng/ml and 4.5 ng/ml for PBS and FBS respectively, thus witnessing that our system can detect CPT-11 at very low concentration levels to cover the entire pharmacokinetic curve.[31]

We also tested SN-38, the active metabolite of CPT-11, as well as the other metabolites SN-38G, APC, NPC to assess whether some effect on AChE activity could be observed, and the results are shown in Supporting Information, Figure S3. The biosensor was activated as described above. However, upon sequential additions of the metabolites, no or negligible change in current response was observed. It is worth mentioning that only SN-38 in the concentration of 1000 ng/ml (2.5 mM) showed an inhibition of 8.9±0.7 % in PBS, and 7.6±0.5% in FBS, for AChE activity. However, SN-38 is usually found at concentration level below 100 ng/ml in plasma samples: while testing this drug dose in the system, the observed inhibition was 7.2±0.6% in PBS and 6.1±0.7%in FBS. Therefore, we can confidently state that SN-38 did not represent a significant interference. The $IC_{50}$ of SN-38 was found to be 0.48 μM (1.9 ng/ml) in PBS and 0.36 μM (1.4 ng/ml) in FBS.

As a final step, we calibrated the biosensors with neostigmine, a powerful reversible inhibitor for AChE that is used in anesthesia. Neostigmine produced an 80% inhibition of the enzymatic activity, thus providing a positive control (Supporting Information, Figure S4).

**Repeatability Test.** The repeatability was evaluated on (i) the performance of the biosensor toward the substrate acetylcholine and (ii) the measurement of CPT-11 concentration. Six biosensors were prepared the same day employing the same batch of reagents and solutions and tested in parallel under identical experimental conditions. The

results are summarized in the Supporting Information, Table S1 and S2.

(i) Concerning the performance of the biosensor toward acetylcholine, $K_M$ and $V_{Max}$ were evaluated using the same concentration of ACh in six replicates. We found an average 13.2% and 14% coefficient of variation (CV%) for $K_M$ and $V_{Max}$, respectively, within an array of eight different biosensors, thus indicating a reliable observed current change (Figure 4b) and an excellent reproducibility in the performance of the biosensor.

(ii) We repeated a calibration test using 10 different increasing CPT-11 concentrations. The results showed excellent back-calculated concentration values within an average imprecision, expressed by CV%, of 9% over six replicates (see Supporting Information, Table S2). Residual enzyme activity was also assessed as 40% in six different biosensors. Nevertheless, we found a discrete variability of the current intensity, measured within 8 biosensors working in parallel (Figure 5). This issue can be ascribed to slightly different surface area for each biosensor, which can be overcome with an automated fabrication process.

**Comparing enzyme-based biosensor with HPLC-MS.** As for comparison, ten calibration standards were analyzed by both the biosensor and the HPLC-MS to assess the quality and performances of our enzyme-based biosensor. In fact, HPLC-MS is considered the reference standard methodology in the analysis of small drug molecules in biological samples, including therapeutic drugs when required by oncologists for specific clinical research programs. The results, summarized in the Supporting Information (Table S3), showed a good correlation between the two techniques with a Pearson coefficient ($R^2$) of 0.9984, as depicted in the Deming plot (Supporting Information, Figure S5). Moreover, such comparison showed an excellent accuracy with respect to HPLC-MS, given the value of 0.998 ± 0.016 for the slope of the linear regression.

**Effect of aging and temperature on biosensor storage.** Furthermore, to assess the stability of the biosensors over time and storing conditions a study on aging was performed on 3 biosensors fabricated following the design **5**. Their performances (in terms of $V_{Max}$ and $K_M$) and stability were checked upon storing at +4, -20 and -80 ºC for a period time ranging from 1 up to 40 days. Results are reported in the Supporting Information, Table S4 and Figure S6.

The best storing condition in terms of stability and performances were attained at -20 ºC. This analysis also evidenced the robustness of the biosensors that can be easily stored dry and used several days after fabrication with minimal loss of sensitivity and performances. Robustness, durability, and reliability of biosensors are rather important features in view of a future application of these tools in TDM at the bedside.

CONCLUSIONS

In this work, we described the fabrication and characterization of an enzymatic biosensor capable of detecting CPT-11 in simple and complex matrices. The biosensor can discriminate between CPT-11 and its metabolites, SN-38, SN-38G, APC, NPC. To the best of our knowledge, this is the first biosensor specifically devised for CPT-11. Our findings showed that CPT-11 can be detected in real time in simple and complex matrix solutions in the clinically relevant range 10-10,000 ng/ml. No or negligible interference by metabolites and co-therapeutic drugs was noted.

Even though the methodology has to be further implemented, validated and engineered, we believe that detecting a new class of antineoplastic drugs is indeed of relevance for the community. Furthermore, thanks to ease fabrication process, robustness, durability, and reliability, the application of such biosensing platform might set the foundation to develop next-generation diagnostics tools aimed at evaluating in real time patients' response to the chemotherapeutic regimen, which might have tremendous fallouts into the clinical practice, the Healthcare System and, most importantly, the quality of life of oncological patients.

Next step of our research work will concern testing the biosensor in human plasma samples, while implementing and engineering the technology to device a portable diagnostic tool. In perspectives, we envision that a point-of-care development and use of such tools in the clinical practice will allow to easily, precisely and rapidly monitoring patients response at the bedside, while reducing dramatically the costs, related to the traditional analytical methods employed in the core facilities. This will be beneficial not only for the Healthcare System, but will also improve the treatment of patients in the developing Countries and remote areas.

## ASSOCIATED CONTENT

### Supporting Information

The Supporting Information is available free of charge on the ACS Publications website. Experimental details; a schematic representation of the biosensor fabrication and summary of designs **1-8**; details on Michaelis-Menten kinetics; biosensor response toward CPT-11 metabolites, SN-38, SN-38G, APC, and NPC; biosensor response toward neostigmine; repeatability test; comparison of enzyme-based biosensor and HPLC-MS (Deming Plot); effect of aging and temperature on biosensors' storage. (PDF)

## AUTHOR INFORMATION

### Corresponding Author

*E-mail: federico.polo@cro.it.
ORCID
Federico Polo: 0000-0003-4638-396X

### Author Contributions

‡These authors contributed equally.

### Notes

The authors declare to have no competing interests

## ACKNOWLEDGMENT

The authors thank Associazione Italiana per la Ricerca sul Cancro (AIRC) for the financial support of this work (Project 12214: Innovative Tools for cancer risk assessment and early diagnosis – 5 x1000).

## REFERENCES

(1) Meneghello, A.; Tartaggia, S.; Alvau, M. D.; Polo, F.; Toffoli, G.

*Curr. Med. Chem.* **2017**, *24*, DOI: 10.2174/0929867324666170720101736..
(2) National Cancer Institute. Alliance for Nanotechnology in Cancer. Develop Small Tools with a Big Impact on Cancer. (Accessed May, 2016).
(3) McKeating, K. S.; Aubé, A.; Masson, J.-F. *Analyst* **2016**, *141*, 429–449.
(4) Kikuchi, N.; Nishiyama, T.; Sawada, T.; Wang, C.; Lin, Y.; Watanabe, Y.; Tamakoshi, A.; Kikuchi, S. *Sci. Rep.* **2017**, *7*, DOI: 10.1038/srep40363.
(5) Kundes, F.; Kement, M.; Cetin, K.; Kaptanoglu, L.; Kocaoglu, A.; Karahan, M.; Yegen, S. F.; Atici, A. E.; Civil, O.; Eser, M.; Cakir, T.; Bildik, N. *Springerplus* **2016**, *5*, DOI: 10.1186/s40064-016-3725-9.
(6) Kawato, Y.; Aonuma, M.; Hirota, Y.; Kuga, H.; Sato, K. *Cancer Res.* **1991**, *51*, 4187–4191.
(7) Wall, M. E.; Wani, M. C.; Cook, C. E.; Palmer, K. H.; McPhail, A. T.; Sim, G. A. *J. Am. Chem. Soc.* **1966**, *88*, 3888–3890.
(8) Kunimoto, T.; Nitta, K.; Tanaka, T.; Uehara, N.; Baba, H.; Takeuchi, M.; Yokokura, T.; Sawada, S.; Miyasaka, T.; Mutai, M. *Cancer Res.* **1987**, *47*, 5944–5947.
(9) Fuchs, C.; Mitchell, E. P.; Hoff, P. M. *Cancer Treat. Rev.* **2006**, *32*, 491–503.
(10) Corona, G.; Elia, C.; Casetta, B.; Toffoli, G. *Ther. Drug Monit.* **2010**, *32*, 638–646.
(11) Capello, M.; Lee, M.; Wang, H.; Babel, I.; Katz, M. H.; Fleming, J. B.; Maitra, A.; Wang, H.; Tian, W.; Taguchi, A.; Hanash, S. M. *J. Natl. Cancer Inst.* **2015**, *107*, DOI: 10.1093/jnci/djv132.
(12) Chabot, G. G. *Clin. Pharmacokinet.* **1997**, *33*, 245–259.
(13) Mathijssen, R. H. J.; Van Alphen, R. J.; Verweij, J.; Loos, W. J.; Nooter, K.; Stoter, G.; Sparreboom, A. *Clinical Cancer Research* **2001**, *7*, 2182–2194..
(14) Rivory, L. P.; Riou, J. F.; Haaz, M. C.; Sable, S.; Vuilhorgne, M.; Commerçon, A.; Pond, S. M.; Robert, J. *Cancer Res.* **1996**, *56*, 3689–3694.
(15) Iyer, L.; King, C. D.; Whitington, P. F.; Green, M. D.; Roy, S. K.; Tephly, T. R.; Coffman, B. L.; Ratain, M. J. *J. Clin. Invest.* **1998**, *101*, 847–854.
(16) Sai, K.; Kaniwa, N.; Ozawa, S.; Sawada, J. I. *Drug Metab. Dispos.* **2001**, *29*, 1505–1513.
(17) Dodds, H. M.; Haaz, M. C.; Riou, J. F.; Robert, J.; Rivory, L. P. *J. Pharmacol. Exp. Ther.* **1998**, *286*, 578–583.
(18) Buck, A.; Halbritter, S.; Späth, C.; Feuchtinger, A.; Aichler, M.; Zitzelsberger, H.; Janssen, K. P.; Walch, A. *Anal. Bioanal. Chem.* **2015**, *407*, 2107–2116.
(19) Kweekel, D.; Guchelaar, H. J.; Gelderblom, H. *Cancer Treat. Rev.* **2008**, *34*, 656–669.
(20) Tsai, H. P.; Lin, L. W.; Lai, Z. Y.; Wu, J. Y.; Chen, C. E.; Hwang, J.; Chen, C. S.; Lin, C. M. *J. Biomed. Sci.* **2010**, *17*, DOI: 10.1186/1423-0127-17-49.
(21) Topkaya, S. N.; Aydinlik, S.; Aladag, N.; Ozsoz, M.; Ozkan-Ariksoysal, D. *Comb. Chem. high throughput Screen.* **2010**, *13*, 582–589.
(22) Litti, L.; Amendola, V.; Toffoli, G.; Meneghetti, M. *Anal. Bioanal. Chem.* **2016**, *408*, 2123–2131.
(23) Vicario, A.; Sergo, V.; Toffoli, G.; Bonifacio, A. *Colloids Surfaces B Biointerfaces* **2015**, *127*, 41–46.
(24) Morton, C. L.; Wadkins, R. M.; Danks, M. K.; Potter, P. M. *Cancer Res.* **1999**, *59*, 1458–1463.
(25) Hyatt, J. L.; Tsurkan, L.; Morton, C. L.; Yoon, K. J. P.; Harel, M.; Brumshtein, B.; Silman, I.; Sussman, J. L.; Wadkins, R. M.; Potter, P. M. *Chem. Biol. Interact.* **2005**, *157–158*, 247–252.
(26) Dodds, H. M.; Rivory, L. P. *Mol. Pharmacol.* **1999**, *56*, 1346–1353.
(27) Badawy, M. E. I.; El-Aswad, A. F. *Int. J. Anal. Chem.* **2014**, DOI: 10.1155/2014/536823.
(28) Lenigk, R.; Lam, E.; Lai, A.; Wang, H.; Han, Y.; Carlier, P.; Renneberg, R. *Biosens. Bioelectron.* **2000**, *15*, 541–547.
(29) Gong, J.; Wang, L.; Zhang, L. *Biosens. Bioelectron.* **2009**, *24*, 2285–2288.
(30) Yang, L.; Wang, G.; Liu, Y. *Anal. Biochem.* **2013**, *437*, 144–149.
(31) Marangon, E.; Posocco, B.; Mazzega, E.; Toffoli, G. *PLoS One* **2015**, *10*, 1–18.
(32) Schuvailo, O. N.; Dzyadevych, S. V.; El'skaya, A. V.; Gautier-Sauvigné, S.; Csöregi, E.; Cespuglio, R.; Soldatkin, A. P. *Biosens. Bioelectron.* **2005**, *21*, 87–94.
(33) Kok, F. N.; Bozoglu, F.; Hasirci, V. *Biosens. Bioelectron.* **2002**, *17*, 531–539.
(34) Tümtürk, H.; Şahin, F.; Demirel, G. *Bioprocess Biosyst. Eng.* **2007**, *30*, 141–145.
(35) Bucur, M. P.; Bucur, B.; Radu, G. L. *Sensors (Switzerland)* **2013**, *13*, 1603–1613.
(36) Rocchitta, G.; Secchi, O.; Alvau, M. D.; Farina, D.; Bazzu, G.; Calia, G.; Migheli, R.; Desole, M. S.; O'Neill, R. D.; Serra, P. A. *Anal. Chem.* **2013**, *85*, 10282–10288.
(37) Rocchitta, G.; Secchi, O.; Alvau, M. D.; Migheli, R.; Calia, G.; Bazzu, G.; Farina, D.; Desole, M. S.; O'Neill, R. D.; Serra, P. A. *Anal. Chem.* **2012**, *84* , 7072–7079.
(38) Monti, P.; Calia, G.; Marceddu, S.; Dettori, M. A.; Fabbri, D.; Jaoua, S.; O'Neill, R. D.; Migheli, Q.; Delogu, G.; Serra, P. A. *Talanta* **2017**, *162*, 151–158.
(39) MacDougall, D.; Crummett, W. B.; et al. *Anal. Chem.* **1980**, *52*, 2242–2249.
(40) International Conference on Harmonisation of Technical Requirements for Registration of Pharmaceuticals for Human Use. ICH Harmonised Tripartite Guideline S7B: The Non-Clinical Evaluation of the Potential for Delayed Ventricular Repolarizatoin (QT Interval Prolongation) by Human Pharmaceuticals.
(41) O'Neill, R. D.; Rocchitta, G.; McMahon, C. P.; Serra, P. A.; Lowry, J. P. *TrAC - Trends Anal. Chem.* **2008**, *27*, 78–88.
(42) Kurbanoglu, S.; Ozkan, S. A.; Merkoçi, A. *Biosens. Bioelectron.* **2017**, *89*, 886–898.

For TOC only

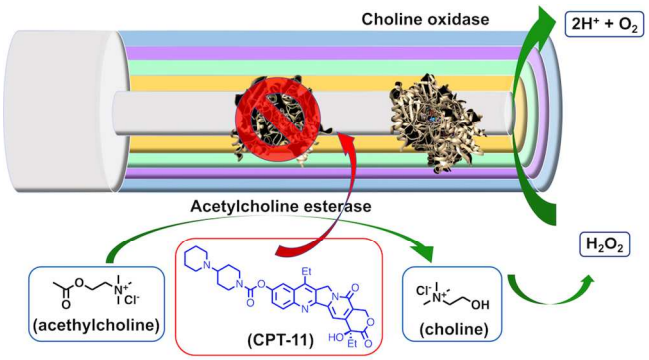
Choline oxidase
2H+ + O2
Acetylcholine esterase
H2O2
(acethylcholine)
(CPT-11)
(choline)